

# Interpreting laboratory liquefaction test results: the importance of confining pressure to unconfined compressive strength ratios

Murray Grabinsky <sup>a,\*</sup>, Mohammadamin Jafari <sup>a</sup>, Ben Thompson <sup>a</sup>, Ryan Veenstra <sup>b</sup>

<sup>a</sup> Paterson & Cooke, Canada

<sup>b</sup> Gold Fields Australia, Australia

## Abstract

*Laboratory liquefaction testing programs on cemented paste backfills (CPBs) have been based on methods used in conventional geotechnical earthquake engineering. The conventional approach emphasises the need to understand the soil's initial state (void ratio and effective confining stress) with respect to the critical state line. Laboratory testing of undisturbed or (more commonly) reconstituted samples is often conducted at an initial effective confining pressure of 100 kPa. There is an assumption in cyclic liquefaction testing that the test results depend on the ratio of cyclic shear stress to initial effective confining stress, regardless of the initial effective confining stress magnitude. However, is this assumption valid for sands (and silts) with artificial cohesion created by binder hydration?*

*The authors recently published a retrospective analysis of monotonic triaxial test results on CPB where both undrained tests with porewater pressure measurements as well as drained tests with volume change measurements were used. It was shown that the ratio of initial effective confining stress to unconfined compressive strength (UCS) can be considered a 'state parameter' used to predict the extent to which porewater pressures (in undrained testing), or volume changes (in drained testing) would develop, regardless of the UCS magnitude. This framework will first be summarised and its application demonstrated to published triaxial test results. Then, the approach is extended to cyclic testing using published test results from both triaxial and simple direct shear testing programs.*

*A major finding from this work is that commonly used heuristics such as "X kPa UCS makes CPB liquefaction resistant" are naive and should be avoided because they do not account for the varying effective confining stress magnitudes that exist in different design scenarios, nor the absolute magnitude of the cyclic shear stress. The findings from this study can also be used to better design future experimental programs to assess cemented paste liquefaction potential for projects both underground and on surface.*

**Keywords:** cemented paste backfill, liquefaction resistance, minimum binder content

## 1 Introduction

Attempts to understand the liquefaction potential of tailings, both cemented and unamended, has taken place within the context of conventional geotechnical earthquake engineering. This has worked well for unamended tailings (i.e. for tailings dams), but the results for cemented tailings have not yielded design tools that can be routinely applied with similar confidence for underground design. There are many factors that contribute to more-challenging liquefaction assessments for underground design, including the complexity of underground geometries for both excavations and rock mass geomechanical domains and features; variations in dynamic loading (amplitude, frequency, duration, and direction of wave propagation); and the influence of binder-induced cohesion on the backfill's fundamental material properties. For unamended

---

\* Corresponding author. Email address: [murray.grabinsky@patersoncooke.com](mailto:murray.grabinsky@patersoncooke.com)

cohesionless natural soils and tailings, it is known that the potential for positive or negative porewater pressure (pwp) development (i.e. contraction versus dilation) during shearing depends on the material's initial state parameter,  $\psi$ , which is the difference between the material's current void ratio and the void ratio at critical state (representing constant volume at large strain shearing) for the given initial effective stress. This concept, arising from critical state soil mechanics, works well in describing cohesionless soil response to undrained shearing under both static (i.e. monotonic axial strain) and dynamic (i.e. cyclic shear) loading. As well, under cyclic shear loading conditions, it is generally accepted that the number of cycles required to induce failure is dependent on the ratio of cyclic shear stress to normal stress, regardless of the normal stress magnitude, and conventionally shear testing is carried out under a 100 kPa confining stress. However, previous studies on cemented backfills (e.g. Pierce 1999) have shown varying amounts of pwp development during undrained monotonic shearing depending on both the cohesion (or, specifically the unconfined compressive strength, UCS) *and* the confining pressure, with all samples being at nominally equal void ratio. This clearly demonstrates the limitations of applying conventional geotechnical earthquake engineering approaches naively to design of underground cemented backfill systems.

Recently, Grabinsky et al. (2025) reassessed the triaxial test results from Pierce (1999) and showed that the extent of pwp development during undrained monotonic shearing (i.e. static testing) could be understood by normalising both shear and confining stresses with respect to the UCS. This results in a new state parameter,  $\chi' = \sigma'/\text{UCS}$ , where  $\sigma'$  is the effective confining stress applied after initial consolidation. For low values of  $\chi'$  (i.e. low confining pressures and high strength) the pwp developed during undrained shearing was small, whereas for higher values (i.e. high confining pressure and low strength) the pwp developed was large. A transitional state was identified at  $\chi'$  between 0.76 and 0.86 where the maximum pwp developed during shear was enough to return the effective stress point at phase transition (the reversal from incremental contraction to dilation) to the same effective stress as the starting condition. The question then arises: can the same approach be used to reinterpret and better understand cyclic shear stress test results on cemented backfill samples?

The question just posed is addressed here using the following approach. The previously cited reinterpreted monotonic test results are summarised to provide the context for the normalisation approach and justification for the proposed new state parameter. Test results from Suazo et al. (2017) are summarised and presented with emphasis on the UCS for each data series tested, and some anomalies are identified. Those test results are then reinterpreted using a modified form of the indicated normalised variables. New insights and interpretations are then made, with recommendations for future work.

## 2 Reinterpreted monotonic test results

Pierce (1999) tested non-plastic gold tailings from Golden Giant mine in monotonic undrained triaxial compression with porewater pressure measurements. The test program involved 3 binder contents and 3 cure times for a total of nine different UCS. For each UCS, triaxial tests were carried out at initial consolidation pressures of about 100, 200, 300, and 400 kPa (approximate conversions from original tests which were controlled in psi Imperial units). Control samples for UCS ranged from 211 kPa (3% binder at 28 days) to 1,029 kPa (7% binder at 115 days). Therefore, the range of initial  $\chi'$  values were from 0.10 (103 kPa confinement/1,029 kPa UCS) to 1.96 (414 kPa confinement/211 kPa UCS). Figure 1 provides examples of deviator stress versus axial strain, and  $p'$ - $q$  stress paths for tests on samples with 3% binder at 28 days (UCS 211 kPa) and 7% binder at 28 days (UCS 457 kPa). Stress paths in this stress space are conventionally called  $s'$ - $t$  to avoid confusion with the definition of  $p'$  and  $q$  based on stress invariants.

Note that all the deviator stress versus axial strain test results shown in Figure 1 show very little strain softening, and so the stress paths are generally monotonically increasing in the  $q$  (or  $t$ ) axis. Therefore, if a steady state line does exist for these materials, the initial states must all lie below the corresponding critical state line. This implies that monotonic liquefaction is not feasible for the given range of test conditions. To better quantify the extent of pwp development during the different tests, each stress path was digitised so that the raw data could be reinterpreted in terms of different stress variables and using different

normalisation processes. The stress paths were then replotted in terms of the normalised variables  $t/UCS$  and  $s'/UCS$  (Figure 2). The  $\chi'$  for each sample corresponds to the  $s'/UCS$  at  $t$  (or  $t/UCS$ ) = 0.

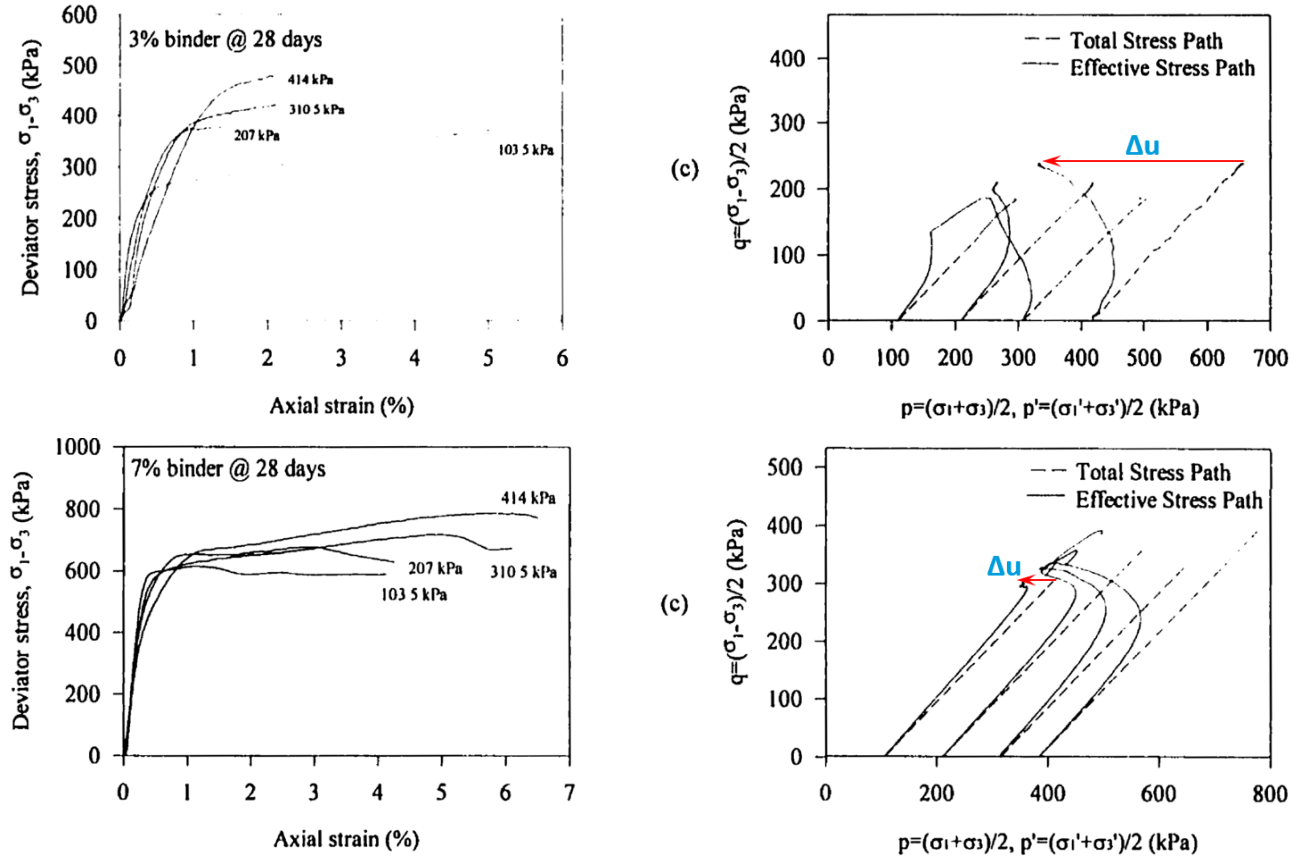


**Figure 1** Examples of test results on cemented paste backfill samples using deviator stress – axial strain plots (left) and stress paths (right) for samples with UCS 211 kPa (top) and 457 kPa (bottom), corresponding to initial  $\chi' = 1.96$  and 0.23. Figures taken from Pierce (1999), with development of maximum pwp superposed

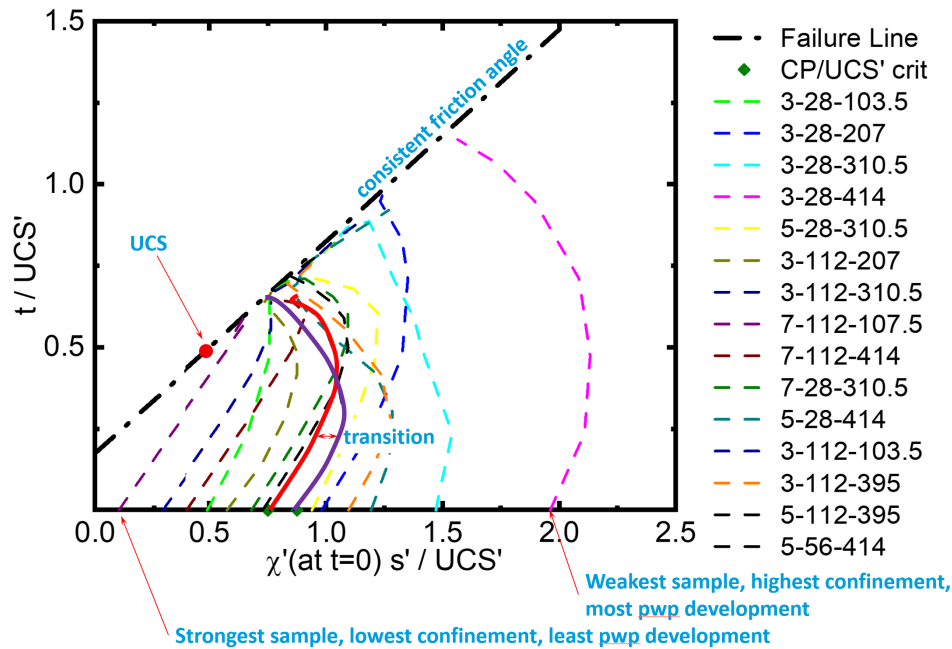


**Figure 2** Stress paths for the samples tested by Pierce (1999) reinterpreted in terms of normalised stress variables

Although none of the samples demonstrated significant strain softening, the extent of pwp generation during shearing can be characterised with respect to the initial  $\chi'$  value. For example, for low  $\chi'$  values there is very little pwp pressure development, and for the smallest ( $\chi' = 0.1$ ), the stress path appears to be monotonic along the  $s'/\text{UCS}$  axis. By contrast, the strongest pwp development occurs for the highest  $\chi'$  value ( $\chi' = 1.96$ ) and at peak pwp development, the  $s'/\text{UCS}$  point on the stress path is less than the starting  $\chi'$  value. To better identify transitions between these 2 extreme behaviours, Figure 3 shows selected stress paths. For  $\chi'$  values up to  $\approx 0.5$  the stress paths increase monotonically as the sample is sheared. Just above  $\chi' \approx 0.5$ , the stress paths reach a maximum  $s'/\text{UCS}$ , and with further shearing, the  $s'/\text{UCS}$  reduces but does not become less than the original  $\chi'$  value. Somewhere between  $\chi' = 0.76-0.86$ , the reduction in  $s'/\text{UCS}$  reaches the original  $\chi'$  value. For larger  $\chi'$  values, the minimum  $s'/\text{UCS}$  on the stress path is less than the original  $\chi'$  value.

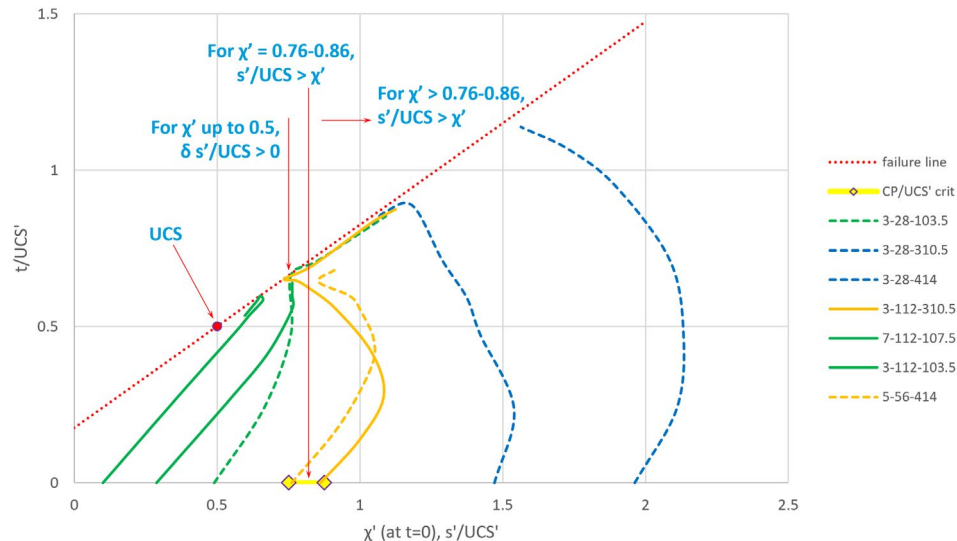


**Figure 3** Selected stress paths showing transitional behaviours in pwp development during shearing

Note that when  $\chi'$  is approximately 0.76 or greater, increasing the initial value of  $s'/\text{UCS}$  leads to higher maximum porewater pressures generated during shearing, which in turn increases the curvature of the resulting stress paths. In addition, the sample may undergo crushing during the initial isotropic compression stage used to raise  $s'/\text{UCS}$  to the target value. Isotropic compression tests conducted by Jafari & Grabinsky (2022) indicate that this pressure is approximately equal to the UCS. Considering this, the first test in which  $s'/\text{UCS}$  exceeded 1 (meaning the effective isotropic pressure surpassed the UCS) corresponds to  $\chi' = 0.76$ . At this point, the likelihood of damage to the cemented bonds increases under both shear loading and isotropic compression, which contributes to the observed escalation in porewater pressure within the sample.

The same normalisation approach can be applied to the total stress analysis results as well. This is shown in Figure 4. For each UCS considered, the corresponding line in the shown stress space represents the total stress failure envelope between the limits of confining pressures used. Therefore, the confining pressures being between about 100 and 400 kPa results in a relatively long failure line for low UCS (i.e. 207 kPa), whereas the failure line appears to be relatively short for the highest UCS (i.e. 1,276 kPa).

Also shown in Figure 4 is the theoretical stress path for a UCS test. This shows that extrapolating the total stress failure envelopes to the theoretical UCS end point will generally result in a value  $t/\text{UCS} = 0.5$  or slightly greater. Therefore, it is reasonable to interpret from this dataset that the undrained shear strength  $C_u = \frac{1}{2}\text{UCS}$ . This analysis and interpretation is probably the strongest evidence available to support the assertion that the undrained shear strength is half the UCS, although this assumption has been commonly used since Mitchell's presentation of it in the analysis of strength requirements for sidewall exposure (Mitchell et al. 1982). Figure 4 also shows that if a total stress analysis is conducted, then a modest undrained friction angle is warranted.

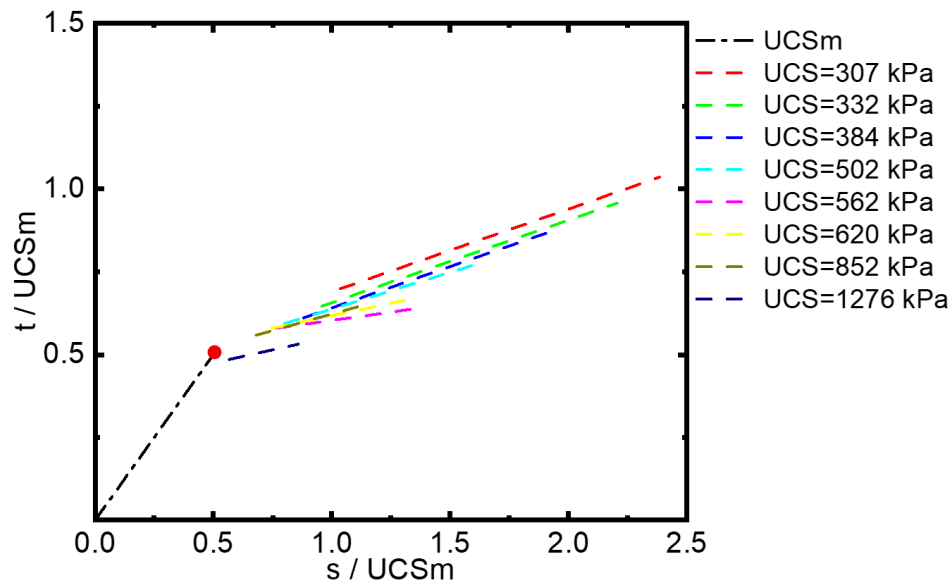


**Figure 4** Total stress failure envelopes (shown only within the limits of the confining pressures used for testing) and theoretical stress path for an UCS test, terminating at (0.5, 0.5) or  $\frac{1}{2}$ UCS

### 3 Direct simple shear test results

Suazo et al. (2017) tested cemented non-plastic tailings with relatively low UCS (less than 132 kPa) using direct simple shear (DSS) equipment and interpreted the test results within the context of a conventional geotechnical earthquake engineering framework. Failure is assessed using the development of either large pwp or large shear strain, although these 2 criterion can be achieved simultaneously in some tests. It is usual for such test results to be presented in terms of the number of cycles required to generate failure for a given shear stress ratio, determined by dividing the applied cyclic shear stress by the initial effective confining stress (conventionally 100 kPa confinement). Curiously, the DSS results were not directly correlated to each test suite's control UCS samples. To reinterpret the Suazo et al. (2017) data, the available figures were digitised and the test suite's corresponding UCS was determined from a separately reported figure. The results of this process are shown in Figure 5. Each of the curves were then best fit with a power function. The coefficients and negative exponents for the power functions were plotted against UCS and power functions best fit to each of these datasets to provide a rational basis for interpolating CSR-N (CSR = cyclic stress ratio) curves for intermediate UCS values (Figure 6). The datasets were then combined, as shown in Figure 7.

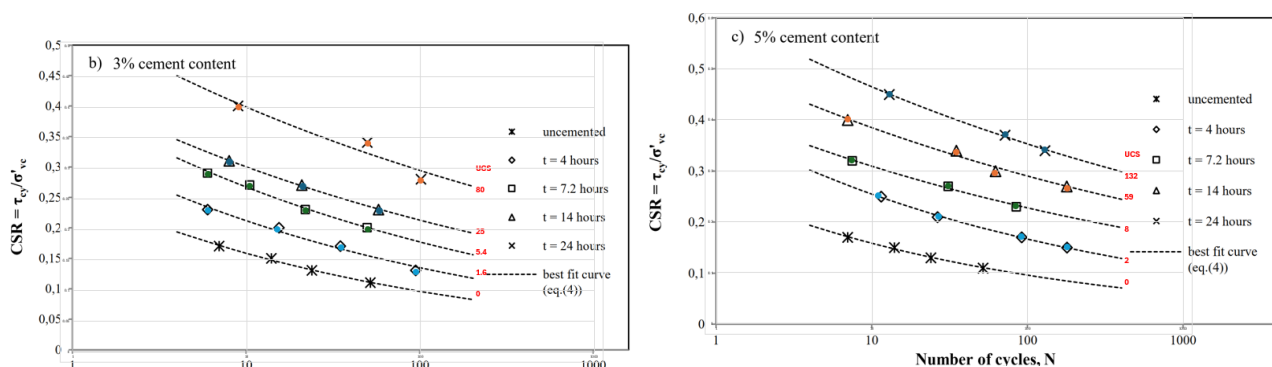


**Figure 5** Digitisation of Suazo et al. (2017) data and correlation with control sample UCS

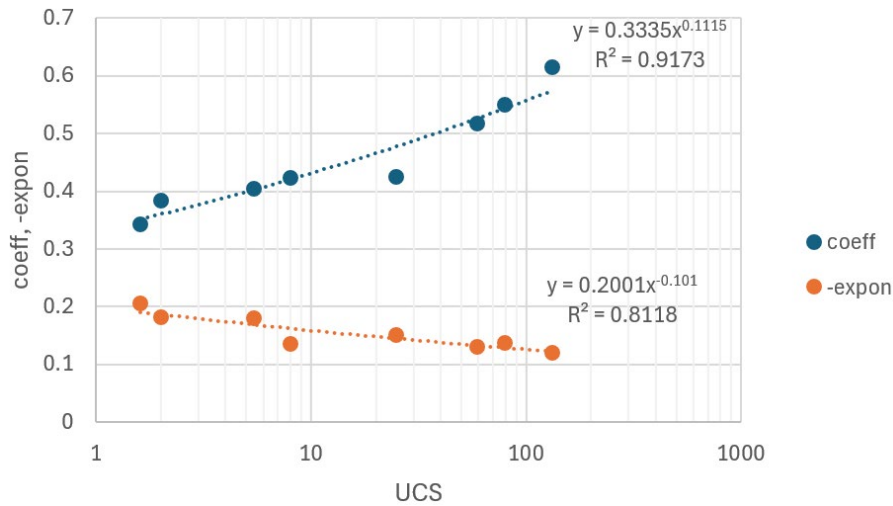


**Figure 6** Coefficients and negative exponents for power functions fit to the original CSR-N curves, plotted against UCS, with fitting functions used to interpolate CSR-N curves for intermediate UCS values

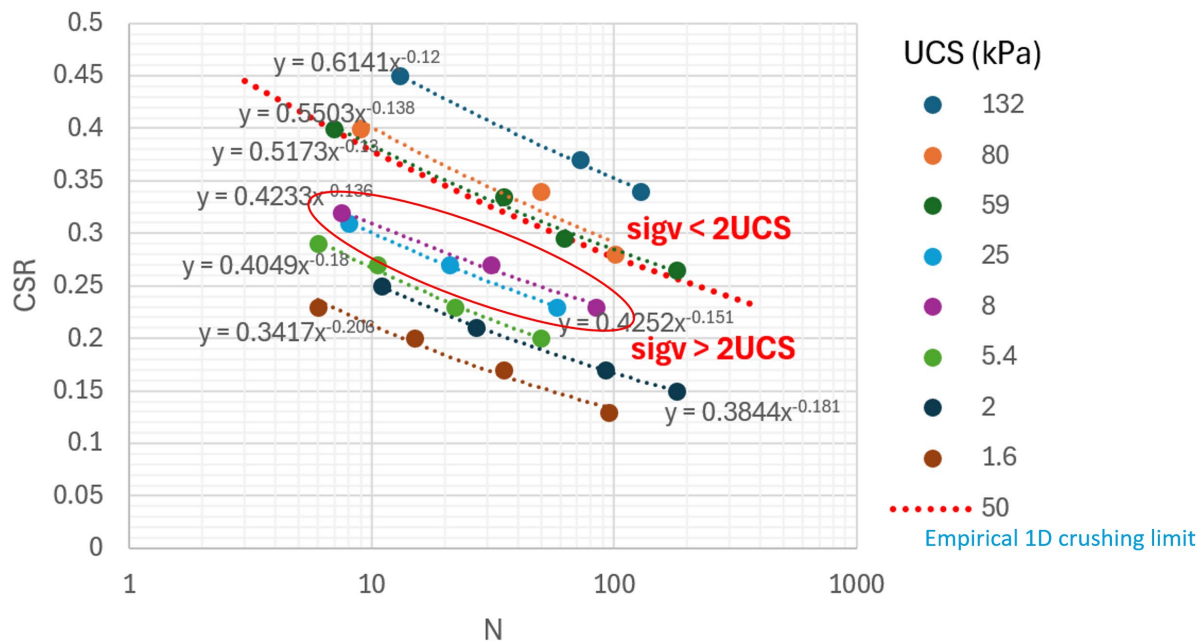


**Figure 7** Combined data with best-fit power CSR-N curve functions; the apparent anomaly between UCS 8 and 25 kPa samples is highlighted in the red ellipse

Conventional oedometer (one-dimensional compression) tests on cemented sands and cemented tailings confirm that significant onset of consolidation settlement occurs when the applied stress reaches about twice the UCS (e.g. Mitchell et al. 1982; Jafari et al. 2020, 2025). Given that Suazo et al. (2017) tested at a normal stress level of 100 kPa, this would mean samples tested with UCS 50 kPa would be on the limit of damage during initial consolidation loading, and weaker samples are increasingly likely to undergo further damage. The results from Figure 6 were used to interpolate the CSR-N curve for 50 kPa UCS, shown as the red dashed line in Figure 7. Note that the location of the CSR-N curve for different UCS values does not appear to strongly correlate with the crushing heuristic (i.e. UCS = 50 kPa). Furthermore, there appears to be an anomaly in the Suazo et al. (2017) results in that the test suite with control sample UCS 8 kPa has a CSR-N curve lying *above* the curve for the suite with control sample UCS 25 kPa, implying that the lower-strength material has higher resistance to liquefaction, which is counterintuitive and not consistent with expected material behaviour. To investigate the details of these test results further, the available data is transformed using the described normalisation approach in the next section.



## 4 Reinterpreted direct simple shear results

As all the DSS tests by Suazo et al. (2017) were conducted at 100 kPa normal stress, it is easy to determine the equivalent cyclic shear stress (i.e. cyclic shear stress = CSR  $\times$  100 kPa). Careful examination of the CRS trend versus UCS in Figure 7 yields a (perhaps) unexpected trend, that the ratio of cyclic shear stress to UCS is decreasing as the UCS increases. Therefore, using the previously suggested normalised stress parameters (i.e. shear\_stress/UCS and normal\_stress/UCS) results in a graphical representation that is counter intuitive. Instead, the inverse of these parameters is used. Compared to Figure 7, the CSR on the vertical axis is replaced with  $UCS/\tau_{cyclic}$ , and the curves are ordered according to  $UCS/\sigma_v$  (where  $\tau_{cyclic}$  represents cyclic shear stress and  $\sigma_v$  represents initially applied normal effective stress). As before, a power function is fit to each resulting curve, and the values of the coefficients and exponents are plotted against  $UCS/\sigma_v$  (Figure 8) to facilitate determining curves for intermediate  $UCS/\sigma_v$  values. Note that the coefficient of determination for the power function fitting the coefficient values is good ( $R^2 = 0.9971$ ), whereas the coefficient for the power function fitting the exponents is less ( $R^2 = 0.81$ ). Compared to the fitting functions for the original dataset (Figure 6) the statistical fit is better for the reinterpreted data ( $R^2 = 0.9971$  versus 0.9173), and the statistical fit for the exponents is virtually identical.

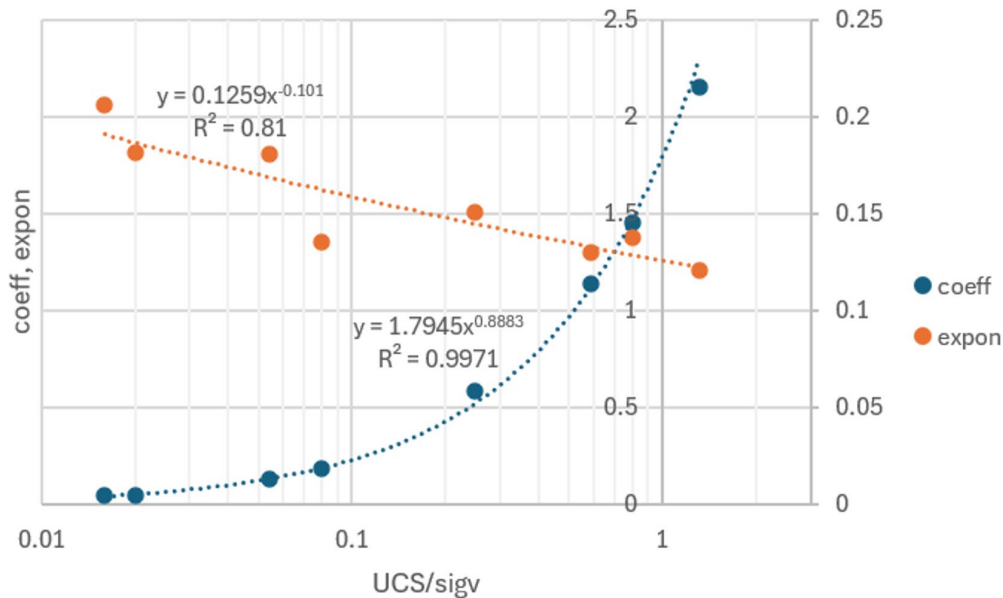


**Figure 8** Coefficients and exponents for power functions fit to the modified curves, plotted against  $UCS/\sigma_v$ , with fitting functions used to interpolate curves for intermediate  $UCS/\sigma_v$  values

The reinterpreted DSS results are shown in Figure 9. The one-dimensional crushing heuristic is again represented by a red dashed line (now with value  $UCS/\sigma_v = 0.5$ ). The data series with  $UCS/\sigma_v > 0.5$  are clearly delineated above this heuristic line; the data series with  $UCS/\sigma_v = 0.08$  and less are clearly clustered at low values of  $UCS/\tau_{cyclic}$  (less than 0.5); and the data series with  $UCS/\sigma_v = 0.25$  (i.e. a value one-half of the crushing heuristic) lies intermediate to these 2 cases. An important interpretation arising from this reanalysis is that the liquefaction resistance of the tested cemented paste backfill *does* depend on the normal stress (vis-à-vis the parameter  $UCS/\sigma_v$ ), which is contrary to the assumption made in liquefaction testing of unamended natural soils and tailings. However, this interpretation needs to be validated through additional laboratory testing.

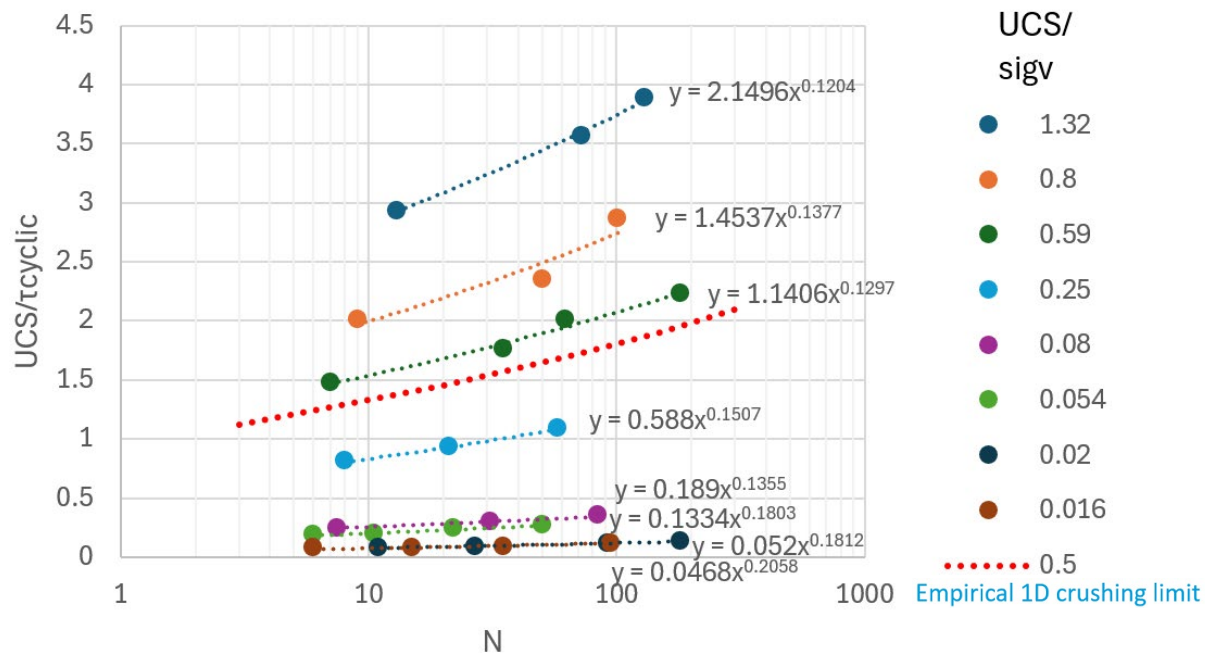


**Figure 9 Reinterpreted direct simple shear results using normalised stress variables**

Suazo et al. (2017) considered an example of strong ground motion involving  $CSR = 0.39$  and 10 cycles of shaking. They plotted  $CSR$  at 10 cycles as a function of  $UCS$  and determined a  $UCS$  in the range of 60–75 kPa represents a value considered resistant to liquefaction. While this example can be considered a worst case scenario because it is based on 10 cycles, it is worth considering what strength might be required in less seismically active regions where both the  $CSR$  and the number of cycles of shaking would be less. For example, Verma et al. (2019) processed seismic records from sites in British Columbia containing low-plasticity soils and developed a relationship between the equivalent number of cycles of uniform shaking and the earthquake magnitude, and showed that their relationship agreed well with previously suggested trends. Extrapolating these trends back to magnitudes in the 3–4 range (the largest ever recorded in Northern Ontario for both mining-induced and naturally occurring earthquakes) suggests  $N = 3$  is appropriate. The reinterpreted results are shown in Figure 10 for  $UCS/\tau_{cyclic}$  as a function of  $UCS/\sigma_v$  at 3 and 10 cycles of shaking, which shows for a given  $UCS/\sigma_v$  the difference in  $UCS/\tau_{cyclic}$  at 3 and 10 cycles is (arguably) not particularly sensitive, but the normalisation process may obscure a better engineering interpretation.

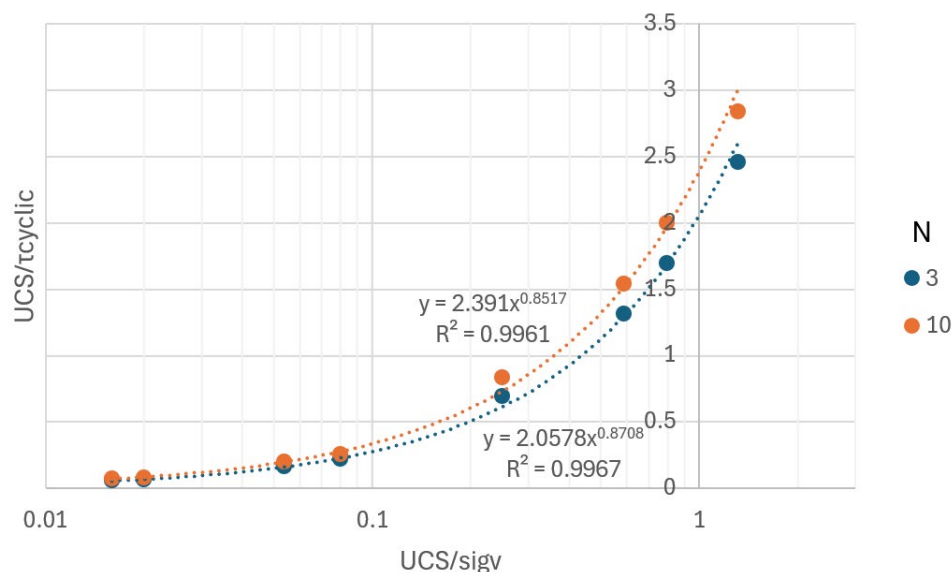


**Figure 10 Results for  $UCS/\tau_{cyclic}$  as a function of  $UCS/\sigma_v$  at 3 and 10 cycles of shaking**



To present the reinterpreted results in a clearer engineering context, Figure 11 shows results for  $\tau_{\text{cyclic}}$  as a function of UCS at different values of effective  $\sigma_v$ , for 3 and 10 cycles of shaking. As all tests were conducted at 100 kPa normal stress, the superposed test data only lie on the  $\sigma_v = 100$  kPa curves. The remaining curves for different values of  $\sigma_v$  are extrapolations outside the range of tested samples, and therefore the hypothesised dependency must be verified using further DSS tests at different normal stress levels. The Suazo et al. (2017) example of  $\tau_{\text{cyclic}} = 39$  kPa (at  $\sigma_v = 100$  kPa) and 10 cycles gives 60 kPa UCS, the lower bound suggested by Suazo et al. (2017). Note that for the same cyclic shear stress but only 3 cycles of shaking, the required UCS drops to 20 kPa – a very different interpretation than made from Figure 10.

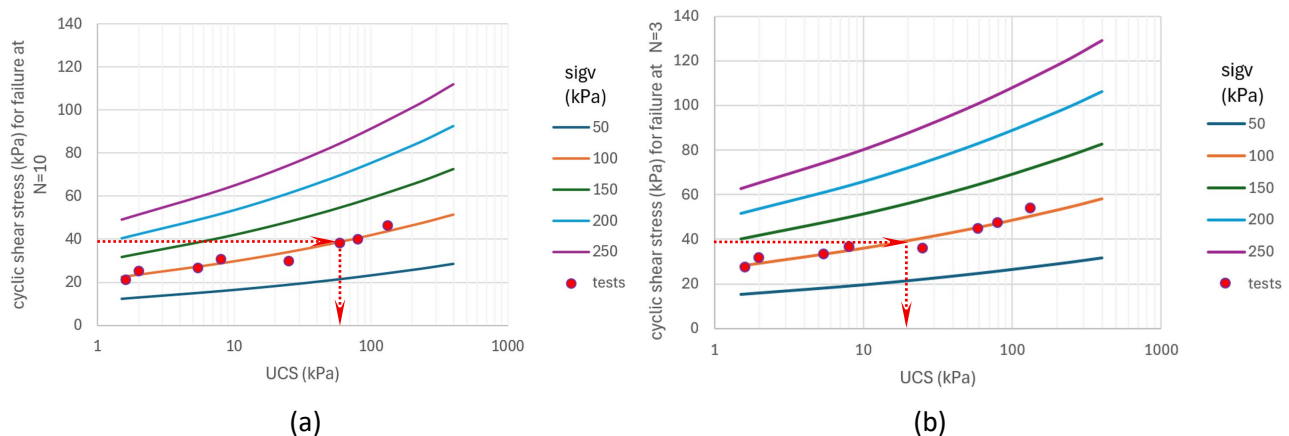


**Figure 11 Results for  $\tau_{\text{cyclic}}$  as a function of UCS at different values of  $\sigma_v$ , for 10 (a) and 3 (b) cycles of shaking**

Note that for a given number of shaking cycles and a given magnitude of cyclic shear stress, the required UCS is sensitive to the initial vertical effective stress. For example, for the shown case of 10 cycles and 39 kPa cyclic shear stress, the required UCS is 60 kPa for  $\sigma_v = 100$  kPa, about 6 kPa at 150 kPa, and less than 2 kPa at 200 kPa. However, at these elevated vertical stress levels with diminishing strengths, the material would strain well beyond the crushing limit, like the lower bound samples in Figure 9. Therefore, once again, the hypothesised dependency must be verified using further DSS tests at different normal stress levels.

## 5 Conclusion

A key takeaway from the analyses presented here is that backfill design engineers (and researchers) need to be more careful when trying to apply conventional geotechnical earthquake engineering concepts to backfill materials with artificially induced cohesion arising from binder hydration. For the triaxial test results presented, the variations in porewater pressure development during shearing cannot be explained based on conventional critical state soil mechanics concepts, as all the samples tested had essentially the same void ratio. Rather, it was shown that a new proposed state parameter  $\chi' = \text{effective confining stress/UCS}$  and normalised stress parameters  $s'/\text{UCS}$  and  $t/\text{UCS}$  satisfactorily explain the observed porewater pressure developed during shearing. The potential for sample crushing during application of the initial confining pressure was also suggested as a key consideration. The observed heuristics can be useful in practical design as well as in developing the experimental design for a new testing program. For example, results from a numerical analysis of a backfill design (almost always a total stress analysis for practical purposes) can be queried to examine the isotropic pressures (or mean stress) compared to the assumed backfill UCS. If the pressures exceed  $\frac{1}{2}\text{UCS}$ , then the developed porewater pressures will be significant enough that perhaps an effective stress analysis needs to be considered. Similarly, if a priori analyses are used to guide the development of a suite of backfill tests, then the range of proposed confining pressures should be compared to the expected range of UCS being tested. This will suggest if any of the tested samples may undergo nonlinear deformation during the application of the confining stress, in which case such samples may be expected to behave differently than stronger samples.

The proposed stress normalisation approach was also successfully applied to the DSS dataset presented by Suazo et al. (2017), albeit using the inverse parameters. This identified a deficiency in the traditional approach of presenting results in terms of the CSR versus number of cycles to failure, in that the magnitude of shear stress vis-à-vis the UCS is important and not captured. The modified approach clearly showed the reduced resistance of samples for which the application of the initial vertical effective stress exceeded the crushing heuristic for one-dimensional consolidation (i.e. significant crushing occurs when  $\sigma_v > 2\text{UCS}$ ). It also successfully resolved the apparent anomaly in the original dataset, for which material with UCS 8 kPa appeared to be more liquefaction resistant than a material with UCS 25 kPa. The modified framework suggests that cyclic shear resistance is sensitive to the magnitude of the applied vertical stress, which is contrary to one of the assumptions in conventional geotechnical earthquake engineering of unamended natural soils and tailings. This remains a hypothesis only, and further laboratory testing is required to determine if this hypothesis is valid, or if the suggested dependency on vertical stress is over-stated. Even within the range of the tested data, however (i.e. at  $\sigma_v = 100$  kPa), it is shown that the required UCS is dependent on the number of cycles to failure (i.e. 60 kPa for 10 cycles versus 20 kPa for 3 cycles). Therefore, much work remains to determine if the currently accepted 'liquefaction limit' (often assumed to be 100–150 kPa) can be rationally reduced for more efficient, yet demonstrably safe mining conditions.

## References

- Grabinsky, M, Jafari, M, Thompson B & Veenstra, R 2025, 'A framework for understanding static liquefaction of tailings with cohesion: insights from cemented backfill', in GW Wilson, DC Sego & J Goodwill (eds), *Proceedings of the Tailings & Mine Waste Conference 2025*, University of Alberta, Edmonton, pp. 1451–1460, <https://tailingsandminewaste.com/conference-proceedings/>
- Jafari, M & Grabinsky, M 2022, 'Predicting the isotropic compression response of hydrating cemented paste backfill', *Journal of Geotechnical and Geological Engineering*, vol. 40, pp. 4821–4836, <https://doi.org/10.1007/s10706-022-02186-7>
- Jafari, M, Shahsavari, M & Grabinsky, M 2020, 'Cemented paste backfill 1-D consolidation results interpreted in the context of ground reaction curves', *Rock Mechanics and Rock Engineering*, vol. 53, pp. 4299–4308, <https://doi.org/10.1007/s00603-020-02173-5>
- Jafari, M, Song, X & Grabinsky, M 2025, 'Development of a method to predict the nonlinear mechanical response of cemented paste backfill to mining induced closure strains', *Rock Mechanics and Rock Engineering*, vol. 58, pp. 9435–9457.
- Mitchell, RJ, Olsen, RS & Smith, JD 1982, 'Model studies on cemented tailings used in mine backfill', *Canadian Geotechnical Journal*, vol. 19, no. 1, pp. 14–28, <https://doi.org/10.1139/t82-002>
- Pierce, ME 1999, *Laboratory and Numerical Analysis of the Strength and Deformation Behaviour of Paste Backfill*, MSc thesis, Queen's University, Kingston, [https://central.bac-lac.gc.ca/.item?id=MQ28246&op=pdf&app=Library&oclc\\_number=46581329](https://central.bac-lac.gc.ca/.item?id=MQ28246&op=pdf&app=Library&oclc_number=46581329)
- Suazo, G, Fourie, A & Doherty, J 2017, 'Cyclic shear response of cemented paste backfill', *Journal of Geotechnical and Geoenvironmental Engineering*, vol. 143, no. 1, [https://doi.org/10.1061/\(ASCE\)GT.1943-5606.0001581](https://doi.org/10.1061/(ASCE)GT.1943-5606.0001581)
- Verma, P, Seidalinova, A & Wijewickreme, D 2019, 'Equivalent number of uniform cycles versus earthquake magnitude relationships for fine-grained soils', *Canadian Geotechnical Journal*, vol. 56, no. 11, pp. 1596–1608, <https://doi.org/10.1139/cgj-2018-0331>